Propagation of extremes in space

C. Nicolis
Institut Royal Météorologique de Belgique, 3 Avenue Circulaire, 1180 Brussels, Belgium

S. C. Nicolis
Department of Mathematics, Uppsala University, P.O. Box 480, SE-751 06 Uppsala, Sweden

(Received 18 February 2009; published 6 August 2009)

The propagation of extreme events in space is analyzed for a class of dynamical systems giving rise to spatiotemporal chaos. It is shown that this process can be mapped into a generalized random walk, whereby the mean square displacement increases linearly in time and there is a nonvanishing probability for jumps beyond first neighbors. The relative roles of the local dynamics and of the spatial coupling are identified.

DOI: 10.1103/PhysRevE.80.026201 PACS number(s): 05.45.−a, 02.50.−r, 05.20.−y

I. INTRODUCTION

There is a growing interest in the study of extreme events in view of their paramount importance in such key areas as global environment, sociology, and finance [1,2]. A variety of methodologies for tackling extreme event-related problems is currently available, from the classical statistical theory [3] to more recent approaches in which the deterministic character of the underlying dynamics is taken into account [4].

Ordinarily when dealing with extremes one focuses on global properties extracted from the available record, among which the statistics of return times or the frequency of level crossings are of special interest. Now, real world systems are extended in space. The relevant issue as far as both prediction and protection are concerned is then not only whether an extreme event will or will not occur globally but, even more so, what is the particular spatial location that will witness at a given time period the occurrence of such an event. This question can be mapped, in turn, into how extremes propagate in space. The objective of the present paper is to outline an approach to this problem for a class of deterministic dynamical systems giving rise to chaotic behavior.

The general formulation is outlined in Sec. II. Sections III and IV are devoted, respectively, to the spatiotemporal dynamics of extremes in spatially extended model systems giving rise to fully developed chaos and to intermittent chaos. Although abstract, these models are prototypical in the sense that they capture the main features of the dynamics under consideration. Emphasis is placed on the relative roles of the strength of spatial coupling and of the local dynamics in the characteristics of extreme propagation. The dynamics of extremes in Fourier space is considered in Sec. V and the main conclusions are summarized in Sec. VI.

II. FORMULATION

Consider a discrete one-dimensional lattice of N spatially coupled elements each described by a continuous variable $x_n(j)$, where n is a discrete time and j is the lattice point. Let $f(x)$ be a function describing the local dynamics and D the coupling constant between a cell located on j with its first neighbors $j \pm 1$. The evolution of $x_n(j)$ is then given by the set of N coupled equations

$$x_{n+1}(j) = f[x_n(j)] + \frac{D}{2}\{g[x_n(j+1)] + g[x_n(j-1)] - 2g[x_n(j)]\}, \tag{1}$$

where g is the coupling function. In the sequel we will adopt the choice $g=f$ frequently made in the literature [5], choose an even number of cells, and write Eq. (1) as

$$x_{n+1}(j) = (1-D)f[x_n(j)] + \frac{D}{2}\{f[x_n(j+1)] + f[x_n(j-1)]\},$$
$$1 \le j \le N. \tag{2a}$$

Unless otherwise specified, periodic boundary conditions will be used throughout and the domain of variation of x and $f(x)$ will be limited to the interval $[a,b]$,

$$x_n(j) = x_n(j+N), \quad a \le x \le b, \quad a \le f(x) \le b. \tag{2b}$$

As mentioned in Sec. I, Eqs. (2) are meant to be prototypical, encompassing large classes of dynamical systems giving rise to complex nonlinear behaviors. In this sense the function $f(x)$ describing the local dynamics is, typically, a one-dimensional endomorphism, as obtained by mapping an underlying continuous time dynamics on a Poincaré surface of section and by subsequently projecting this mapping along the most unstable direction of the motion. The choice of nearest-neighbor coupling is motivated by the fact that most of the continuous time models representing real world physicochemical systems are in the form of partial differential equations involving the nabla or the Laplace operators which, once discretized in space, couple any given point to its first neighbors only. More involved couplings including global ones may be used when modeling networks such as neural nets, information systems, or social systems. They give rise to interesting behaviors, including partial or total synchronization [6], which are out of the scope of this work since the dynamics of extremes becomes then rather straightforward.

Among the different properties of the spatiotemporal dynamics generated by Eq. (2), we are interested here in the instantaneous location of the largest value of $x_n(j)$ observed in the lattice, $M_n(i) = \max\{x_n(j)\}$. The question we address is how $M_n(i)$ will propagate in space, i.e., how the lattice site i bearing initially $(n=0)$ the largest value observed instanta-

 ©2009 The American Physical Society

neously on the lattice will move time going on. We will proceed by mapping this question into a problem of generalized random walk [7], in which the main quantity of interest is the jump Δr_m (in multiples of the lattice distance) accomplished at intermediate times $m=1,2,\ldots,n$, the total displacement realized at the observation time n being

$$r_n = \sum_{m=1}^{n} \Delta r_m$$

$$\text{with } r_n^2 = \sum_{m=1}^{n} \Delta r_m^2 + \sum_{m \neq m'=1}^{n} \Delta r_m \Delta r_{m'}. \tag{3}$$

Given the probability density $P(\Delta r)$ and other statistical properties of Δr, the objective is then to derive the behavior of the displacement r_n as a function of the coupling constant and of the parameters built in the iterative mapping $f(x)$.

To get a feeling on the role of the local dynamics it is instructive to consider briefly, as a reference, the case of N uncoupled ($D=0$) elements in each of which x is the outcome of a process of uniform noise. Clearly, the displacements Δr are then uniformly distributed with a probability distribution, mean, and variance given by

$$P(\Delta r) = \frac{1}{N}, \quad 0 \leq \Delta r \leq N-1, \quad \text{mod}\frac{N}{2},$$

$$=0, \quad \text{otherwise},$$

$$\langle \Delta r \rangle = 0,$$

$$\langle \Delta r^2 \rangle = \frac{1}{N}\left[\sum_{j=1}^{N/2} j^2 + \sum_{j=1}^{N/2-1} j^2\right] = \frac{N^2+2}{12}, \tag{4}$$

where in writing the last relation care was taken to avoid double counting of the cell $1 \equiv N+1$. Applied to Eq. (3) these relations yield

$$\langle r_n \rangle = 0,$$

$$\langle r_n^2 \rangle = n\langle \Delta r^2 \rangle = n\frac{N^2+2}{12} \tag{5}$$

since the individual Δr_m's are here independent ($\langle \Delta_m \Delta r_{m'} \rangle = 0$) and identically distributed random variables. It follows that the position of the instantaneous maximum undergoes as far as its second moment is concerned a random walk with an effective "diffusion" coefficient

$$d = \frac{N^2+2}{24} = \frac{\langle \Delta r^2 \rangle}{2}.$$

As an example for $N=50$ one gets $\langle \Delta r^2 \rangle = 208.5$ and $d = 104.25$.

III. FULLY DEVELOPED SPATIOTEMPORAL CHAOS

In this section we consider the spatiotemporal dynamics of maxima in systems operating in the regime of fully developed chaos. Clearly, the spatial mobility of the maximum will be conditioned by the two following factors: (i) its sojourn probability on the cell in which it originally occurred; (ii) the extent to which the coupling D limits the range and frequency of jumps between the different lattice points visited consecutively by it.

The first of these factors depends essentially on the nature of the local dynamics and, in particular, on the location of the image and preimages of the region close to the maximum value $x=b$. We shall first consider the uncoupled case ($D=0$) in which the mobility coefficient can be computed analytically, and perform subsequently numerical simulations confirming the theoretical predictions in this limit and extending them to the analytically intractable case of nonzero coupling.

A. Logistic maps

As a first representative model we consider a lattice of logistic maps. Consider the local dynamics in absence of coupling,

$$x_{n+1} = 1 - \alpha x_n^2, \quad -1 \leq x_n \leq 1, \tag{6}$$

with $\alpha=2$. Clearly, if set initially to a value close to 1 (its maximum value), the variable x is bound to evolve to a value close to -1 in the next iteration. The sojourn probability of maximum in the cell $j=0$ on which it initially occurred is thus zero and, starting from this cell, jumps of all possible magnitudes to the other cells are equally probable:

$$P(\Delta r) = 0, \quad \Delta r = 0,$$

$$= \frac{1}{N-1}, \quad \Delta r \neq 0. \tag{7}$$

The variance of Δr is given by

$$\langle \Delta r^2 \rangle = \frac{1}{N-1}\left[\sum_{j=1}^{N/2} j^2 + \sum_{j=1}^{N/2-1} j^2\right]$$

or, comparing with Eq. (4),

$$\langle \Delta r^2 \rangle = \frac{N}{N-1}(\langle \Delta r^2 \rangle)_{\text{uniform noise}}. \tag{8}$$

Figure 1 depicts the probability density of the jumps Δr as obtained from the numerical solution of the full set of equations (2) for $N=50$ and f given by Eq. (6). The full line in Fig. 1 stands for the limiting case of uncoupled cells leading to a distribution of Δr in full agreement with the analytic result of Eq. (7). The dashed line pertains to the opposite case of strong coupling. The distribution of Δr develops now a more intricate structure reflected by strong selection rules whose expected overall result is to enhance the mobility of the maximum. This is confirmed by Fig. 2(a), in which the behavior of the mean square distance as a function of time n, $\langle r_n^2 \rangle$, is summarized. The full line in the figure refers to the uncoupled case $D=0$. It is a straight line whose slope, equal to ≈ 213, is again in full agreement with analytic result of Eq. (8). For reference the result pertaining to 50 uncoupled

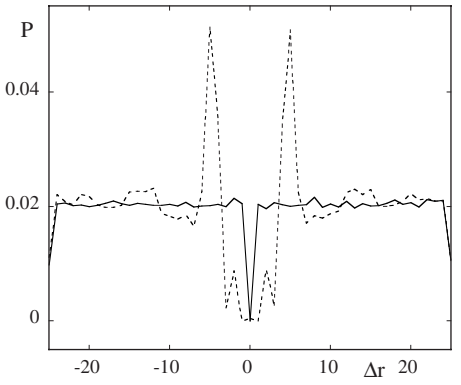

FIG. 1. Probability of jumps Δr (in multiples of the lattice distance) from the cell containing initially the largest value of x as obtained numerically from Eq. (2) with $N=50$ and f given by Eq. (6). The (dimensionless) coupling constant D is $D=0$ (full line) and $D=0.95$ (dashed line). Number of realizations is 10^5.

cells each undergoing a uniform noise process is also depicted (open circles) revealing a slope of ≈ 208.5 in full agreement with Eq. (5). Switching on a nonzero coupling (dashed and dotted lines in the figure) keeps the behavior still diffusive since the corresponding curves are straight lines but the overall mobility tends to be enhanced as anticipated in the comments made in connection with Fig. 1. There is nevertheless some variability around this general trend as seen in Fig. 2(b), where the slopes (or equivalently the mobilities) are plotted against the coupling coefficient D. The origin of this variability is to be sought in the complexity of the phase diagram of the dynamical system defined by Eqs. (2) and (6). In particular, detailed analysis reveals the presence of period 2 (in both space and time) windows for values of D close to 0.2, 0.7, and 0.8. Clearly in the vicinity of the corresponding bifurcation points transport is bound to be more sluggish and this is indeed reflected by the decreasing trends seen in these regions in Fig. 2(b).

The diffusive character of the propagation of the maximum has been further confirmed by the computation of higher moments of r_n and of its probability distribution (not shown). As it turns out the skewness is zero for all n's and the kurtosis tends rapidly to zero, whereupon the probability distribution becomes Gaussian.

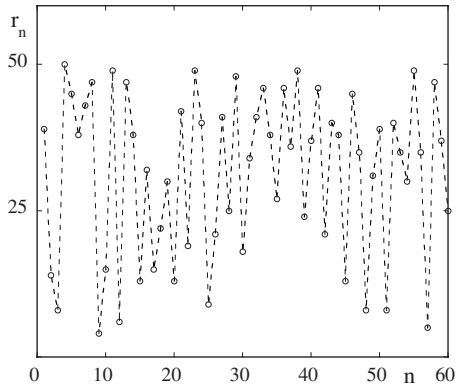

FIG. 3. Time evolution of the location r_n (in multiples of the lattice distance) of the cell containing the maximum value of x for the model of Fig. 1 with $D=0.05$.

Figure 3 shows a time series of successive values of the instantaneous position r_n of the maximum for weakly coupled logistic maps. As can be seen the evolution is quite irregular. To test statistical independence of the successive events we use the method of contingency tables combined with a χ^2 test [8]. The analysis reveals that to the 5% level, contrary to a record generated by random noise, the time series of Fig. 3 is correlated.

B. Bernoulli maps

We next turn to a lattice of Bernoulli maps. The local dynamics in the absence of coupling is now given by

$$x_{n+1} = 2x_n \mod 1 \quad 0 \le x \le 1. \tag{9}$$

Contrary to the logistic map, starting with x close to its maximum $x=1$ favors the occurrence of x values in the same range, entailing that there is now a nonvanishing sojourn probability of the maximum in the starting cell. As a result, the mobility of the maximum is expected to decrease compared to both the uniform noise and logistic cases, despite the fact that the invariant probabilities of x for uniform noise and for the Bernoulli system are identical. Clearly, we have here a signature of the deterministic character of the process.

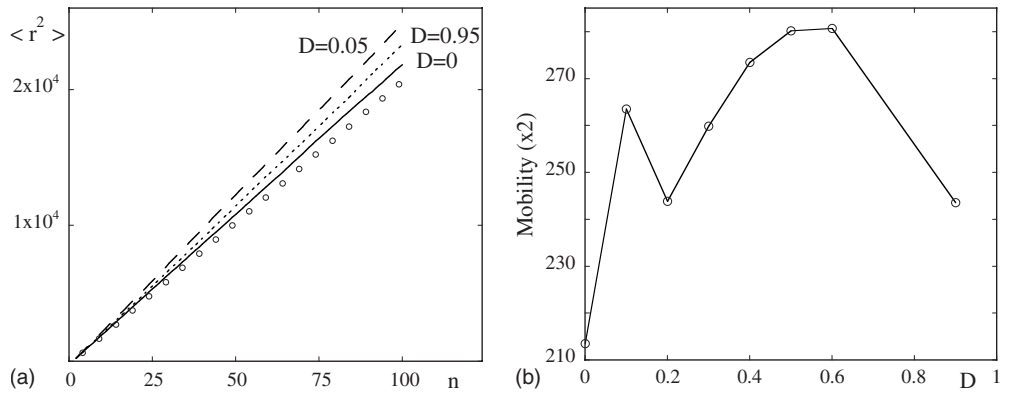

FIG. 2. (a) Time evolution of the mean square displacement (multiples of the lattice distance squared) of the largest value of x [Eq. (3)] for the model of Fig. 1 for different values of the (dimensionless) coupling constant D. Empty circles stand for the behavior of a uniform noise on the same interval. (b) Dependence of the associated mobility coefficient of the extreme on coupling D.

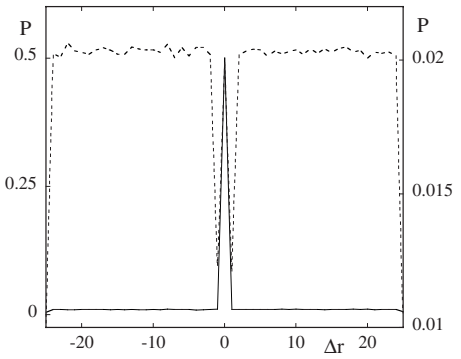

FIG. 4. As in Fig. 1 with f given by Eq. (9). Right ordinate stands for the case of $D=0.95$.

To obtain a quantitative estimate we partition the unit interval into K equal cells (which constitutes a Markov partitioning) and agree to regard the rightmost cell $C_M=(1-1/K,1)$ as the interval of variation of the maximum. After one iteration this cell will be mapped into $f(C_M)=(1-2/K,1)$ such that (a), $f(C_M)$ contains C_M entirely; and (b), the measure of the intersection $f(C_M)\cap C_M$ is equal to that of the complement C'_M of C_M in $f(C_M)$. It follows that the *a priori* probabilities of the maximum to remain in C_M or to leave it are both equal to 1/2. In the event that the maximum will leave C_M, in the absence of coupling jumps of all possible magnitudes to the other cells will be equally probable. This leads to the following form of the jump probability $P(\Delta r)$:

$$P(\Delta r) = \frac{1}{2}, \quad \Delta r = 0,$$

$$= \frac{1}{2(N-1)}, \quad \Delta r \neq 0. \tag{10}$$

The variance $\langle \Delta r^2 \rangle$ corresponding to this distribution is

$$\langle \Delta r^2 \rangle = \frac{1}{2(N-1)} \left[\sum_{j=1}^{N/2} j^2 + \sum_{j=1}^{N/2-1} j^2 \right] \tag{11}$$

or, comparing with Eq. (7),

$$\langle \Delta r^2 \rangle = \frac{1}{2} (\langle \Delta r^2 \rangle)_{\text{logistic}} = \frac{N}{2(N-1)} (\langle \Delta r^2 \rangle)_{\text{uniform noise}}. \tag{12}$$

In Fig. 4 the probability densities of Δr as obtained from the numerical solution of the full set of equations (2) for $N=50$ and f given by Eq. (9) are shown. In the uncoupled cell case (full line) full agreement with the analytic result of Eq. (10) is obtained. In the opposite limit of strong coupling (dotted line, $D=0.95$), one obtains a more intricate dependence indicating that jumps to all cells except to the nearest and to the farthest ones of the reference cell may occur with practically equal probabilities (dotted line). The behavior of the mean square displacement $\langle r_n^2 \rangle$ of the maximum as a function of time, for different coupling strengths, is summarized in Fig. 5(a). In all cases a straight line indicative of diffusive behavior is observed. In the limit of uncoupled cells ($D=0$) the slope of this line is in full agreement with the estimate of Eq. (11). As D is gradually switched on, the slope—and thus the mobility of the maximum—is practically increasing monotonously (contrary to the logistic map case), as seen in Fig. 5(b) where the mobility is plotted against D. For strong couplings [$D=0.95$, dotted line in Fig. 5(a)] the result becomes indistinguishable from that corresponding to uncoupled cells undergoing a uniform noise process. The computation of higher moments and of the probability distribution of r_n confirms the diffusive character of the process, which is asserted after a short transient stage during which the kurtosis takes nonzero values.

Finally, the time series of successive values of the instantaneous position r_n of the maximum (not shown) has similar properties as in the logistic map case. In particular, the successive values are statistically correlated.

IV. INTERMITTENT CHAOS

We shall now extend the analysis of the preceding section to account for the presence of more intricate forms of chaos. Specifically, we consider N spatially coupled cells [Eq. (2)] in each of which the local dynamics described by the mapping $f(x)$ is intermittent as a result of the marginal stability [slope of $f(x)$ equal to 1] of one of its fixed points. Without loss of generality, the latter will be chosen to lie on one (or

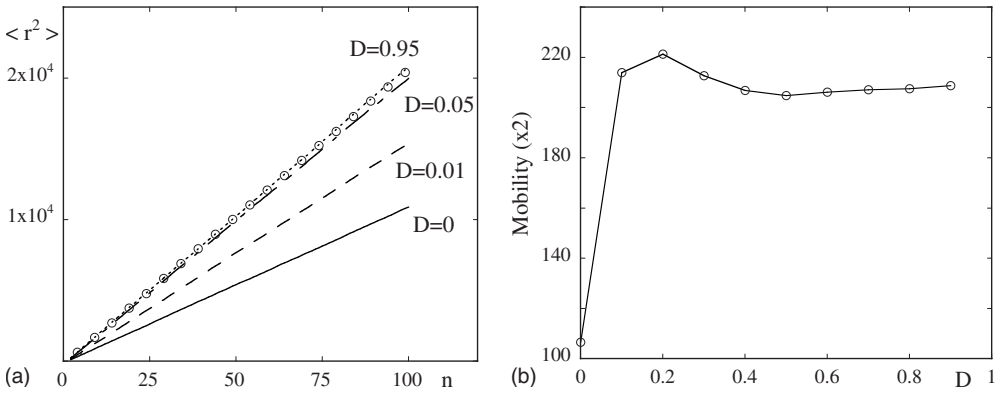

FIG. 5. (a) As in Fig. 2(a) with f given by Eq. (9). (b) As in Fig. 2(b) with f given by Eq. (9).

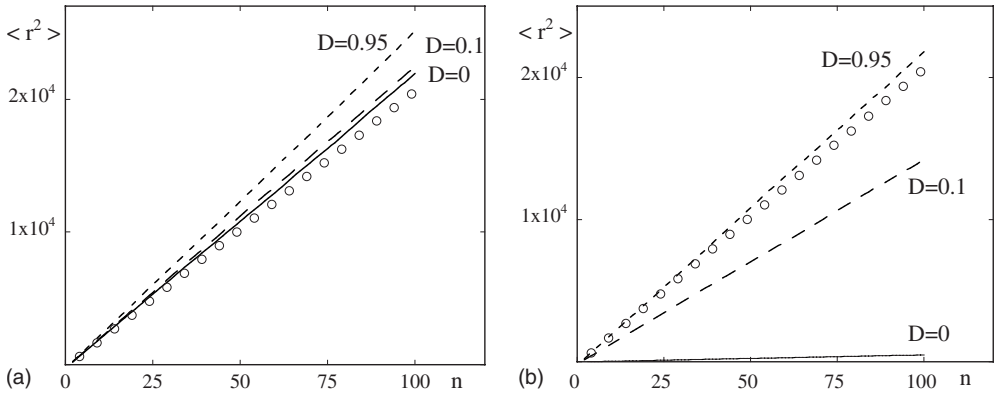

FIG. 6. As in Fig. 2(a) with f given by (a), Eq. (14a) and (b), Eq. (14b).

both) the end points a and b of the domain of variation of x and $f(x)$ close to which the map will then have the limiting form [9]

$$f(x) = x + \mu(x-a)^z \quad x \to +a \tag{13}$$

and similarly for $x \to -b$ if b happens to be a tangency point, with $z > 1$.

Intuitively, for weakly coupled cells one expects that if the laminar region is limited to the neighborhood of the leftmost point the sojourn time of the extreme (bound to be close to b) in the cell in which it is initially observed will be very small. As a result, the mobility of the extreme will be large. Conversely, if the neighborhood of the rightmost point b happens to be a laminar region the sojourn time will be large and the mobility will be small. With increasing values of the coupling constant D the nature of the local dynamics will be altered and, in the strong coupling limit, the situation is expected to be not very different from the one described in the preceding section.

In the sequel we confront these qualitative predictions with the numerical study of two representative examples of intermittent chaos, whose study will also reveal some further interesting trends:

(i) the symmetric cusp map

$$f(x) = 1 - 2|x|^{1/2}, \quad -1 \le x \le 1 \tag{14a}$$

for which $x=-1$ is the (unique) marginally stable fixed point;

(ii) the antisymmetric cusp map

$$f(x) = 1 - 2|x|^{1/2}, \quad -1 \le x \le 0,$$

$$= -1 + 2|x|^{1/2}, \quad 0 < x \le 1. \tag{14b}$$

for which both $x=-1$ and $x=1$ are marginally stable fixed points. In either case the limiting form of $f(x)$ around -1 and/or 1 is as in Eq. (13) with an exponent z equal to $z=2$.

Figures 6(a) and 6(b) depict the behavior of the mean square distance $\langle r_n^2 \rangle$ as a function of n for maps (14a) and (14b), respectively. In both cases the behavior is essentially diffusive, at least up to times $n \approx 10^2$, but there are marked differences in the mobility of the maxima. In the symmetric map [Eq. (14a)] the mobility of the maximum in absence of coupling ($D=0$, full line) is higher than the one obtained for an equal number of uncoupled cells each undergoing a uniform noise process (open circles) the opposite being true in the antisymmetric map [Eq. (14b)], in full agreement with the prediction advanced earlier in this section. As the coupling strength is increased the mobility is increasing in a practically monotonic fashion for both the symmetric and the antisymmetric case as seen in Fig. 7, where the mobilities are plotted against D. In the limit of strong coupling the behavior is practically indistinguishable from the case of fully developed chaos, a fact that is further reflected by the coincidence for all practical purposes of the corresponding probability distributions of displacements Δr (not shown).

The persistence of the maximum in a given cell conditioned by its initial occurrence in this cell in the antisymmetric cusp case is further illustrated in Fig. 8. It takes its most pronounced form in absence of coupling (full line) and still holds albeit in a milder form up to moderate couplings (dotted line). Clearly, we are here in presence of a highly correlated process compared to the behavior depicted in Fig. 3.

V. EXTREME DYNAMICS IN FOURIER SPACE

In spatially extended systems it is often useful to expand the variables in series of linearly independent functions incorporating symmetry properties and boundary conditions. Arguing in terms of the expansion coefficients—the modes—rather than the original variables allows then one to capture collective properties that would otherwise remain blurred, especially if eventually the essence of the dynamics

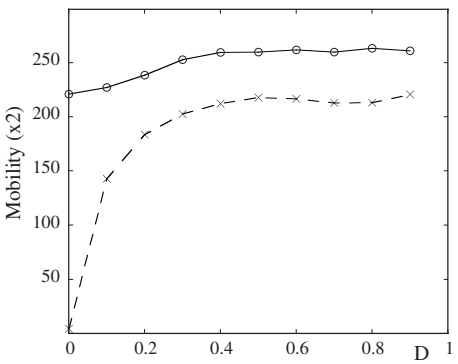

FIG. 7. As in Figs. 2(b) and 5(b) with f given by Eq. (14a) (empty circles) and Eq. (14b) (crosses).

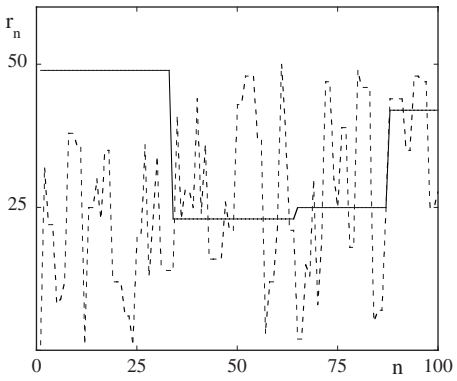

FIG. 8. Time evolution of the location r_n (in multiples of the lattice distance) of the cell containing the maximum value of x for the antisymmetric cusp map [Eq. (14b)] with $D=0$ (full line) and $D=0.1$ (dashed line).

turns out to be borne by a limited number of modes. The objective of this section is to study how the extreme value dynamics is projected into the different spatial modes of the coupled map system described by Eq. (2).

In view of the boundary conditions adopted a Fourier expansion appears to be the most adequate one,

$$a_k = \frac{1}{N}\sum_{j=1}^{N}\left(\cos\frac{2\pi}{N}kj + i\,\sin\frac{2\pi}{N}kj\right)x(j), \quad (k=0,\ldots,N-1). \tag{15}$$

Among the different a_k's, a_0 and $a_{N/2}$ are real and correspond to the space average and to the fastest space-varying combination of the $x(j)$'s, respectively,

$$a_0 = \frac{1}{N}\sum_j x(j), \tag{16a}$$

$$a_{N/2} = \frac{1}{N}\sum_j \cos\,\pi j x(j) = \frac{1}{N}[-x(1)+x(2)-x(3)+\cdots]. \tag{16b}$$

All other modes are complex conjugate, with

$$\mathrm{Re}\ a_k = \mathrm{Re}\ a_{N-k}, \quad 1 < k < \frac{N}{2}. \tag{17}$$

Furthermore, a_0 and $a_{N/2}$ are the only modes containing combinations of *all* the variables present.

Consider now Eq. (2) in the weak coupling limit. Two cases may be distinguished:

Case 1. The probability density associated to the iterative mapping $f(x)$ (assumed to fulfill sufficiently strong ergodic properties) has its maximum (or takes at least appreciable values) in both the neighborhood of the rightmost point b, where the extreme of x is expected to occur, and that of the leftmost point a. This is what happens, for instance, in the logistic map for $\alpha=2$ and in the antisymmetric cusp map. It follows that the probabilities of having all $x(j)$'s close to their extremum or half of them close to it and the other half close to their minimum are appreciable. In turn, the corresponding values for a_0 and $a_{N/2}$ will be comparable and large with an appreciable probability, and larger than the values of the other modes owing to the absence of some of the $x(j)$'s in the latter. This prediction is confirmed entirely by the results of the numerical evaluation of the modes using Eqs. (2) and (15), reported in Figs. 9(a) and 9(b) for the logistic and the antisymmetric cusp maps, respectively. As the coupling D is gradually increased the selection becomes increasingly sharper in the logistic map case: mode a_0 imposes itself as the main bearer of the extreme dynamics, while the role of $a_{N/2}$ and even more so that of the other modes is becoming increasingly weak. The selection is milder in the antisymmetric cusp map case, where it tends to enhance the role of large spatial scales (small k's).

Case 2. The probability density of $f(x)$ is a decreasing function of x, taking its smallest values in the neighborhood of the point where the extreme of x is occurring. This is what happens, in particular, in the symmetric cusp map. It follows that the probability of having all $x(j)$'s close to their extremum (here $x=1$) is very small or, alternatively, that mode a_0 is essentially not populated. Conversely, the probability of having the odd-numbered cells close to their smallest value (here $x=-1$) leaving the even-numbered cells to an interval of values close to the mean is appreciable. It follows that

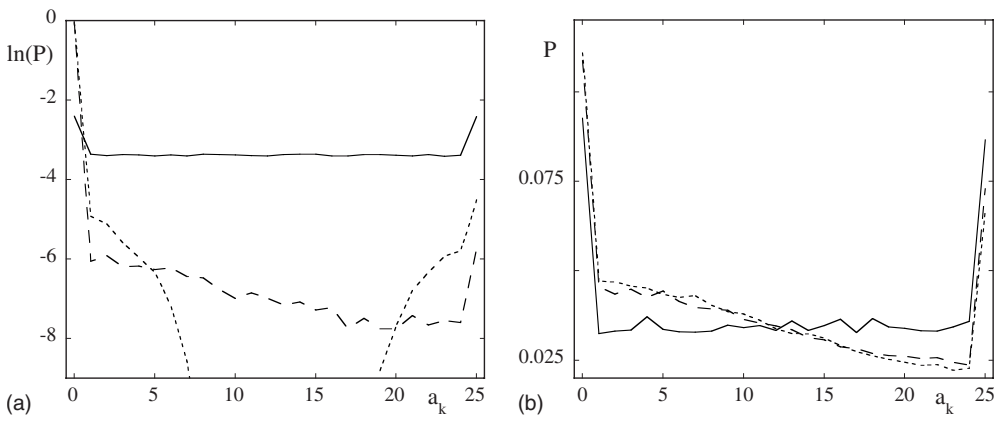

FIG. 9. Probability density of extremes in the Fourier space with $N=50$ and three different (dimensionless) coupling coefficients $D=0$ (full line), $D=0.1$ (dashed line), and $D=0.95$ (dotted line) as obtained numerically for the logistic map (a) and the antisymmetric cusp map (b). Modes for which P is strictly zero [modes 9 to 19 in case (a) and $D=0.95$] are omitted in the corresponding graphs.

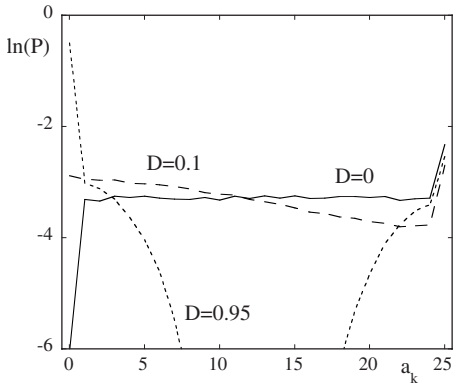

FIG. 10. As in Fig. 9 but for the symmetric cusp map.

mode $a_{N/2}$ is populated appreciably and becomes thus the main carrier of the extremes in Fourier space, since as noticed earlier the other modes contain a lesser number of $x(j)$'s. Again, this is confirmed entirely by the results of the numerical evaluation depicted in Fig. 10. Notice that as D is increased the mode a_0 is becoming increasingly relevant and, in the strong coupling limit, it is the main carrier of the extremes. In this particular range the dynamics of the full system of coupled cells becomes, naturally, quite different from that of the single map looking in fact closer to what is happening in case 1.

As a corollary of the foregoing one expects that the sojourn probability of the extremum on mode a_0 (if started initially on this state) will be substantial in case 1, the opposite being true for mode $a_{N/2}$ as soon as the coupling D reaches appreciable values and for mode a_0 in case 2. This is confirmed by the results of numerical evaluation starting from the full set of equations (not shown).

VI. CONCLUSIONS

The propagation of extremes in space is of central importance in the problematics of prediction of complex systems. In this work we have analyzed some features of this process for prototypical classes of dynamical systems giving rise to spatiotemporal chaos. Our main conclusion has been that propagation can be viewed as a generalized random walk, sharing with classical random walk the property that the mean square displacement increases linearly in time but differing from it by the possibility of performing a wide range of jumps to both near and far neighbors. We have identified the probability density of these jumps as well as the effective mobility of the extreme and disentangled the relative roles of the local dynamics and of the spatial coupling.

An important consequence of the diffusive character of propagation of extremes in space is that long-range connections can be established in a rather short time interval. This should be taken into account when attempting to predict their future evolution.

Throughout the present work the parameters controlling the system's behavior were taken to be space and time independent. Furthermore, the system was supposed to be free of systematic external forcings. Now, the occurrence of extreme events in many real world situations is often accompanied by the presence of systematic biases giving rise to a statistically nonstationary process, for instance, suddenly switching on an electronic circuit or a strong depression invading a previously quiescent atmosphere. It would undoubtedly be interesting to extend our analysis to account for such situations. The extension to space and time-continuous models of concrete systems arising in environmental or in physicochemical applications would also be worth undertaking.

ACKNOWLEDGMENT

This work was supported in part by the Human Frontiers Science Programme.

[1] E. Montroll and W. Badger, *Introduction to Quantitative Aspects of Social Phenomena* (Gordon and Breach, New York, 1974).
[2] *Climate Extremes and Society*, edited by H. F. Diaz and R. J. Murnane (Cambridge University Press, Cambridge, 2008).
[3] P. Embrechts, P. Küppelberg, and T. Mikosch, *Modeling Extremal Events* (Springer, Berlin, 1999).
[4] C. Nicolis, V. Balakrishnan, and G. Nicolis, Phys. Rev. Lett. **97**, 210602 (2006); C. Nicolis and S. C. Nicolis, Europhys. Lett. **80**, 40003 (2007).
[5] K. Kaneko, Physica D **34**, 1 (1989).
[6] V. Anishchenco, V. Astakhov, A. Neiman, T. Vadivasova, and L. Schimansky-Geier, *Nonlinear Dynamics of Chaotic and Stochastic Systems* (Springer, Berlin, 2002).
[7] E. Montroll and G. Weiss, J. Math. Phys. **6**, 167 (1965).
[8] A. Papoulis, *Probability and Statistics* (Prentice-Hall, New Jersey, 1990).
[9] T. Geisel and S. Thomae, Phys. Rev. Lett. **52**, 1936 (1984).